Edited by J.F. Nie, A.J. Morton and B.C. Muddle

Effect of Strain per Pass on Formation of Texture and Microstructure during Asymmetrical Rolling in AA 1050

M-Y. Huh[1], Y-K. Jee[1], J-C. Lee[1], O. Engler[2]

[1] Division of Materials Science and Engineering, Korea University, Seoul 136-701, Korea
[2] Hydro Aluminium Deutschland GmbH, R&D Center Bonn, P.O. Box 2468, D–53014 Bonn, Germany

Keywords: Asymmetrical rolling, Shear texture, Strain state, FEM simulation

Abstract

Asymmetrical rolling was performed by rolling AA 1050 sheets with different velocities of upper and lower rolls. The effect of the reduction per rolling pass on the formation of textures and microstructures during asymmetrical rolling was studied. In order to intensify the shear deformation, asymmetrical rolling was carried out without lubrication. The strain states associated with asymmetrical rolling were investigated by simulations with the finite element method (FEM). A fairly homogeneous net shear strain throughout the sheet thickness was observed after asymmetrical rolling. Asymmetrical rolling with a large reduction per a pass led to a stronger texture gradient in the sheet thickness.

1. Introduction

The strain state accompanying normal symmetrical rolling is commonly simplified by a plane strain state (e.g. [1]). Under the plane strain state, the typical rolling texture comprised of the copper-orientation {112} <111>, S-orientation {123}<634> and brass-orientation {011}<211>, also known as the β-fiber, develops in cold rolled aluminum sheets [2, 3]. Rolling without lubrication gives rise to a deviation from the plane strain state, which leads to the formation of shear textures in thickness layers close to the sheet surface [4, 5]. Asymmetrical rolling, that is rolling with different roll speeds or different roll diameters, increases the shear strain rate components during rolling, which may provide the formation of shear textures throughout the whole thickness layers of rolled sheets [6].

Since the deformation geometry of the roll gap depends on the reduction during the rolling pass, the strain state throughout the thickness layers strongly varies with the reduction per rolling pass. A large reduction per pass along with high friction between roll and sample gives rise to a strong variation of the strain state through the sheet thickness, which results in pronounced texture gradients [7].

In this work, asymmetrical rolling was performed by rolling commercial purity aluminum with different upper and lower roll velocities. In order to investigate the effect of the reduction per pass, samples were asymmetrically cold rolled according to three different routes to the same final thickness.

The formation of texture and microstructure in the asymmetrically cold rolled samples was investigated at various through-thickness layers. The strain state during asymmetrical rolling was analyzed by the finite element method (FEM).

2. Experimental Procedures

The as-received material was 6 mm thick hot band of the commercial aluminum alloy AA 1050. To prepare samples for the asymmetrical rolling trials, the hot band was subjected to an anneal at 260 °C for 1 h. These initial samples were asymmetrically cold rolled according to three different processing routes to a final thickness of 3 mm. *Route 1*: The strip was rolled from 6 to 3 mm in a single pass. *Route 2*: The sample was rolled in two passes, 6 → 4.5 → 3 mm. *Route 3*: The sample was rolled by three passes, 6 → 5 → 4 → 3 mm. The upper and lower rolls had the same roll diameter of 150 mm, yet rolling was performed with different roll velocities; the velocity of the upper roll was 1.5 times faster than that of the lower roll. Note that the asymmetrical rolling experiments in this work were performed without lubrication so as to enlarge the shear deformation.

For macro-texture analysis, pole figure measurements were carried out by means of a conventional X-ray texture goniometer [8]. Various through-thickness layers of the sheets were prepared by careful grinding, polishing and etching of the sheets down to the layer of interest. In the following, the sheet layers are indicated by the parameter *s*, with *s*=+0.9, *s*=+0.5, *s*=0.0, *s*=-0.5, and *s*=-0.9 denoting the layer close to the upper surface, mid-thickness layer between the upper surface and sheet center, sheet center layer, mid-thickness layer between the lower surface and sheet center, and layer close to the lower surface, respectively.

3. Experimental Results and Discussion

The as-received hot band displayed a typical rolling texture composed of the β-fiber orientations at all positions through the thickness. In order to produce an initial material with a more homogeneous microstructure and texture, the hot band was subjected to anneal at 250 °C for 1 h, and from this annealed material the initial samples for the asymmetrical rolling experiments were prepared. During the anneal the hot band experienced a notable softening from Hv=45 to 35, while the texture remained virtually unchanged. Figure 1 shows examples of textures of the hot band and initial sample.

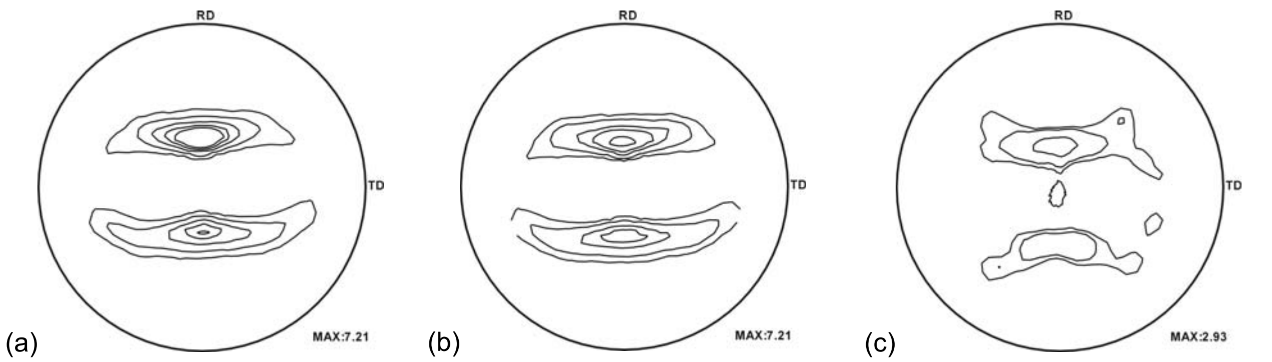

Figure 1: {111} pole figure showing textures of (a) hot band sample, *s*=0.9, (b) initial sample, *s*=0.9, (c) initial sample sample, *s*=0.0.

Figure 2 shows the evolution of texture during asymmetrical rolling in one pass (i.e. following *route 1*). Unlike the initial samples, the asymmetrically rolled sample displayed a strong texture gradient. Typical shear texture orientations with a strong {001}<110> were found in the upper and lower surface layers (*s*=+0.9 and -0.9). The center layer (*s*=0) and the mid layer (*s*=-0.5) between the lower surface and sheet center displayed the typical rolling texture of the β-fiber orientations. The texture of the mid-thickness layer (*s*=+0.5) between the upper surface and sheet center comprised a mixture of rolling texture and shear texture component. Thus, asymmetrical rolling with large draughts led to an asymmetrical distribution of textures throughout the sample thickness.

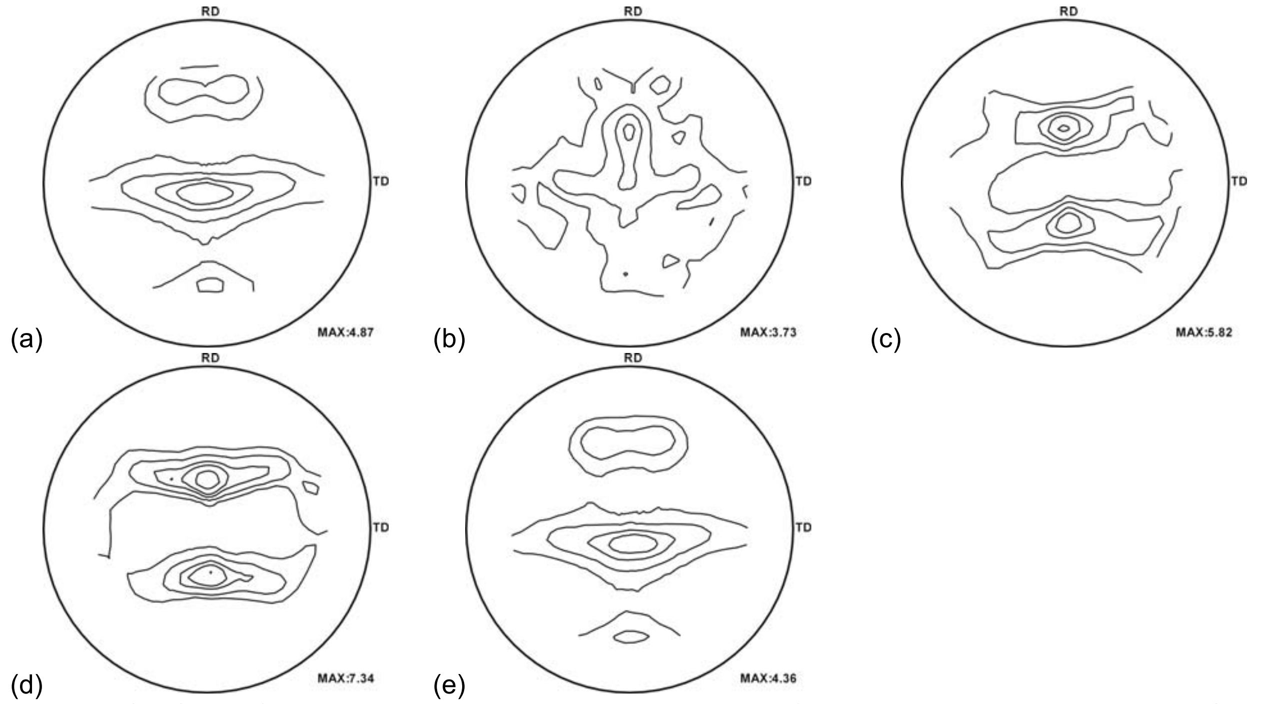

Figure 2: {111} pole figures showing through-thickness textures after asymmetrical rolling in *route 1* (cold rolled in a single rolling pass. (a) *s*=+0.9, (b) *s*=+0.5, (c) *s*=0.0, (d) *s*=-0.5, (e) *s*=-0.9.

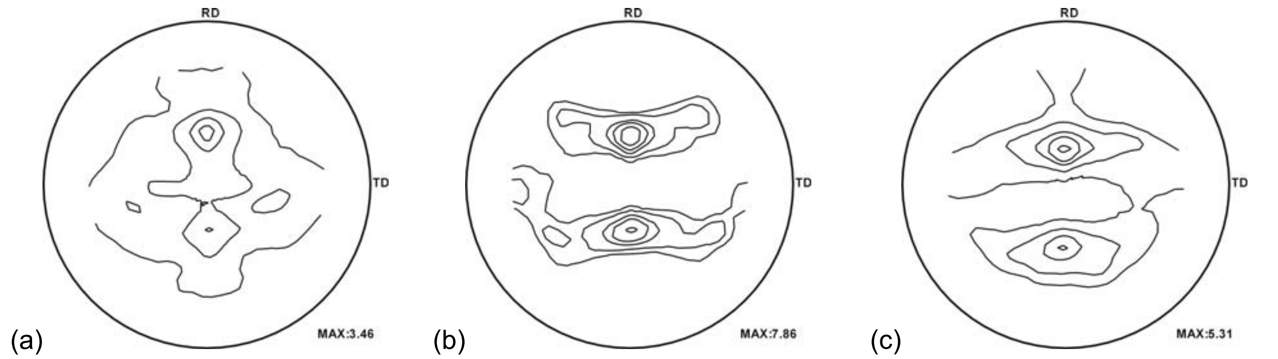

Figure 3: {111} pole figures showing through-thickness textures after asymmetrical rolling in *route 2* (cold rolled in two rolling passes). (a) *s*=+0.9, (b) *s*=0.0, (c) *s*=-0.9.

After asymmetrical rolling by *route 2* (i.e. deformed by two rolling passes) shear texture components developed only in the upper surface layer (*s*=+0.9) in contact with the faster upper roll, while the other thickness layers displayed textures close to the rolling texture. Interestingly, asymmetrical rolling according to *route 3* (i.e. rolled by three rolling passes) led to the formation of a rolling texture throughout the whole thickness layers. It was found that after asymmetrical rolling the texture intensity of the rolling texture increased in thickness layers displaying the rolling texture.

The results of the texture experiments are summarized in Table 1. From the present work, two points should be noted. (i) Asymmetrical rolling with a large reduction per rolling pass leads to the preferential formation of shear texture components in thickness layers close to the sheet surface, while asymmetrical rolling with a small reduction per pass gives rise to the evolution of the rolling textures as in a symmetrical cold rolling. (ii) The formation of shear textures is preferred in the surface layer in contact with the faster roll than that in contact with the slower roll.

Table 1: Summary of texture evolution after asymmetrical rolling (shear and rolling denote shear texture and rolling texture, respectively).

	S=+0.9	*s*=+0.5	*s*=+0.0	*s*=-0.5	*s*=-0.9
Route 1	shear	shear+rolling	rolling	rolling	shear
Route 2	shear+rolling	rolling	rolling	rolling	rolling
Route 3	rolling	rolling	rolling	rolling	rolling

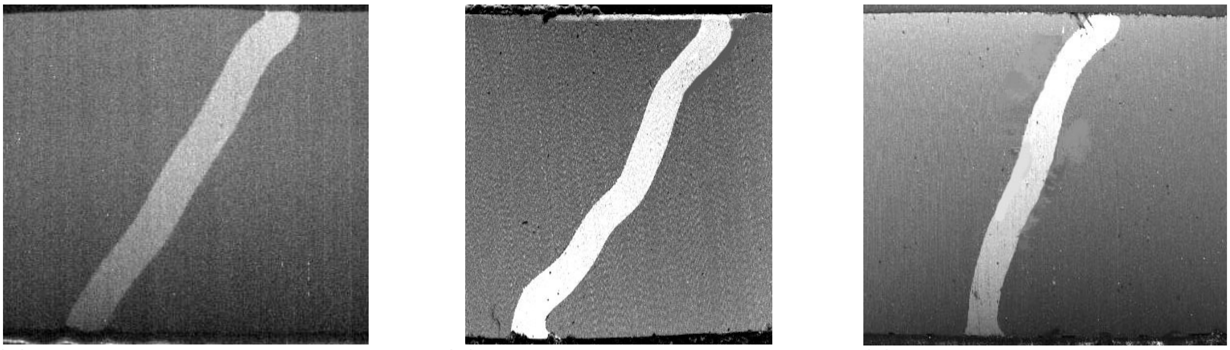

(a) *route 1* (b) *route 2* (c) *route 3*

Figure 4: Changes in the strain marking (vertical prior to asymmetrical rolling) after asymmetrical rolling.

Our recent work [9] has shown that strain marking experiments may well be used to draw conclusions on the overall strain state. For the strain marking experiments a copper wire with a diameter of 0.3 mm was vertically inserted in the initial sample sheet. Figure 4 displays the changes in the position of the marker after asymmetrical rolling. Apparently, asymmetrical rolling led to a rotation of the (originally vertical) wire about the transverse direction. Comparison of the three routes shows that the angle of rotation decreases with decreasing strain per rolling pass from ~32° in *route 1* to 30° in *route 2* to 20° in *route 3*. These rotations are indicative of a net shear strain e_{13} after deformation is finished.

In normal symmetrical rolling, the shear strain component e_{13} strongly depends on the through thickness position, in particular during rolling with high friction. In such instances, the amount of the net shear strain at the surface layers is commonly larger than that of the center layer, which results in a characteristic C-shape of the strain markings. In contrast, the present results demonstrate that a fairly homogeneous net shear strain can be obtained by asymmetrical rolling. However, a homogeneous net shear strain e_{13} throughout the thickness does *not* imply that the shear component of the velocity gradient $\dot{e}_{13}$ – which affects the evolution of the deformation texture – has to be homogeneous throughout the sample thickness.

Since the changes in net strain and the resulting texture evolution are controlled by the strain history in the roll gap, the variation of the strain state throughout the sheet thickness was simulated by means of the rigid-plastic FEM code DEFORM [10]. The FEM simulations were performed on a mesh of 6500 initially square-shaped elements. As in the experimental set-up, the sheet was deformed in one, two, or three bites from 6 to 3 mm; the roll diameter of the rolls was 150 mm and the circumferential roll speed of upper and lower rolls was 150 and 100 mm/s, respectively.

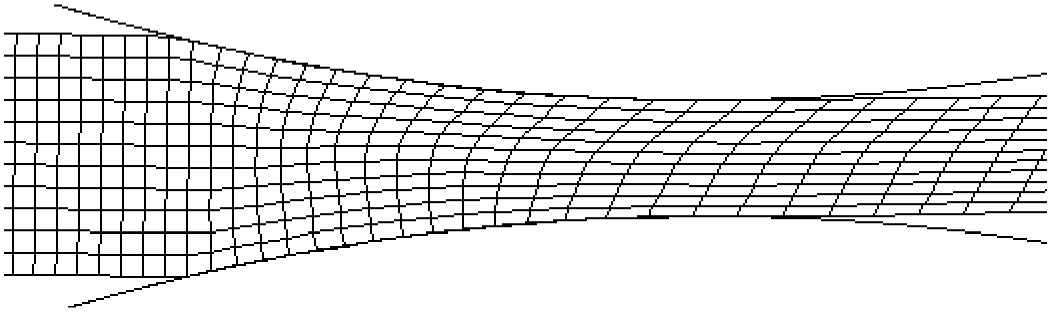

Figure 5: Changes in FEM mesh during the asymmetrical rolling pass in *route 1.*

In the FEM simulation of the strain state during rolling knowledge about the friction between rolls and sheet is vital. As outlined in Ref [9], the friction coefficient can be estimated from a series of careful strain marking experiments. In the present study it turned out that the friction between the (faster) upper roll and the sample was higher than that between the (slower) lower roll and the sample. An example of changes in FEM mesh during asymmetrical rolling is shown in Figure 5. In case of asymmetrical rolling in *route 1*, the combination of μ=0.3 between upper roll and sample and μ=0.2 between lower roll and sample provides the best fit between experimental strain markings (Figure 4 (a)) and simulated FEM mesh (Figure 5). It was found that applying a slightly lower friction condition resulted in a better FEM simulation in *route 2* and *3*.

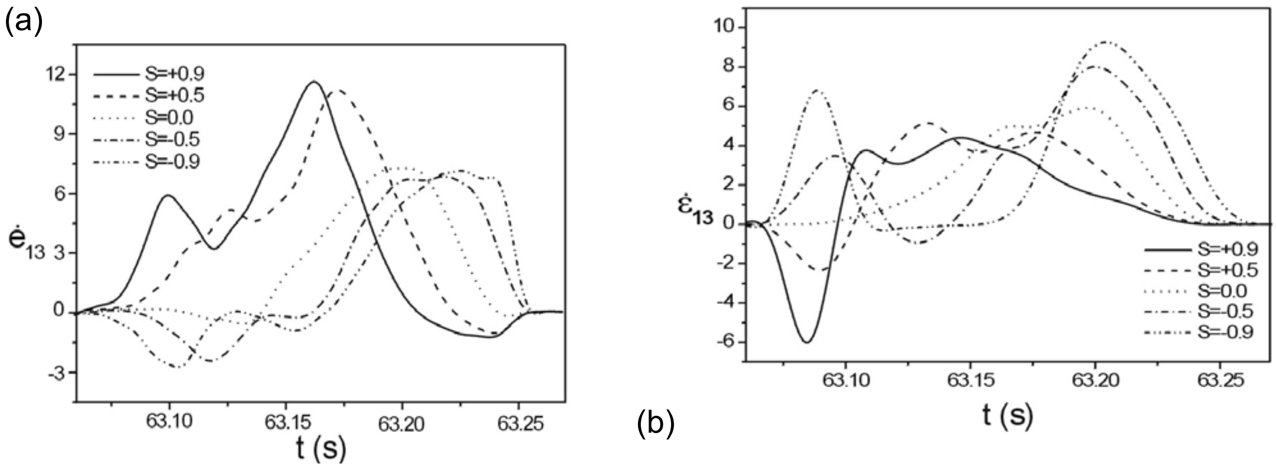

Figure 6: Variations of (a) $\dot{e}_{13}$ and (b) $\dot{\varepsilon}_{13}$ in a roll gap during asymmetrical rolling in *route 1*.

Figure 6(a) shows the variation of the strain rate component $\dot{e}_{13}$ along the streamline for five different layers of *s*=+0.9, +0.5, 0.0, -0.5, and -0.9 during asymmetrical rolling in *route 1* (rolled in one pass). Apparently, $\dot{e}_{13}$ varies from the entrance to the exit of the roll gap and also in the various thickness layers. The net shear strain e_{13} of each thickness layer can readily be obtained by integration of $\dot{e}_{13}$ over each streamline. The amount of e_{13} at *s*=+0.9 is somewhat larger than that at *s*=-0.9, which reflects a slightly larger net shear angle at *s*=+0.9 than at *s*=-0.9 as observed in the experimental strain marking in Figure 4(a) and in the FEM mesh in Figure 5. Note that the net shear strain is fairly uniform throughout the whole thickness layers and has a positive value of e_{13} in all thickness layers, resulting in the shape of the strain marking observed in Figure 4(a).

The evolution of deformation texture is largely controlled by the strain rate $\dot{\varepsilon}_{ij}$, which is the symmetrical part of the velocity gradient $\dot{e}_{ij}$. Figure 6(b) shows a strong dependence of the shear strain rate component $\dot{\varepsilon}_{13}$ on the thickness layers. The layers *s*=+0.9 and -0.9 close to the sheet surface display a larger variation of $\dot{\varepsilon}_{13}$ than the sheet interior (*s*=+0.5, 0.0 and -0.5). It has repeatedly been demonstrated that a large variation of $\dot{\varepsilon}_{13}$ related to the overall thickness reduction $\dot{\varepsilon}_{33}$ gives rise to the evolution of shear textures, while strain states with a small $\dot{\varepsilon}_{13}$ result in the formation of the typical rolling texture [1, 4, 5]. The surface layers of the asymmetrically rolled sample in *route 1* indeed displayed shear textures. Accordingly, the present work disclosed that strong texture gradients developed even in the sample displaying a fairly homogeneous net shear strain after asymmetrical rolling.

Microstructural observations with TEM and EBSD revealed that sub-grains formed more frequently in the thickness layers close to the sheet surface than in the sheet interior. A higher hardness in the surface layers than in the sheet center also reflected this result. However, the effect of the strain per rolling pass could not be observed in the microstructure.

4. Summary

The effect of the reduction per rolling pass on the formation of textures and microstructures during asymmetrical rolling was studied in AA 1050 sheets. Asymmetrical rolling with different roll velocities resulted in a fairly homogeneous net shear strain along the sheet thickness. However, asymmetrical rolling with a large reduction per pass led to a large variation of the shear component $\dot{\varepsilon}_{13}$, which consequently gave rise to the evolution of a strong texture gradient throughout the various thickness layers.

Acknowledgement

This work was supported by grant No. R01-2001-000-00261-0 from the Korean Science and Engineering Foundation.

References

[1] O. Engler, M.Y. Huh and C.N. Tomé, Metall. Mater. Trans. A, 31A, 2299-2315, 2000.
[2] J. Hirsch and K. Lücke, Acta Metall., 36, 2863-2883, 1988.
[3] M.Y. Huh, S.Y. Cho and O. Engler, Mater. Sci. Eng., A315, 35-46, 2001.
[4] M.Y. Huh, J.C. Park and S. Lee, Met. & Mater. Inter. 2, 141-149, 1996.
[5] O. Engler, H.C. Kim and M.Y. Huh, Mater. Sci. Technol., 17, 75-86, 2001.
[6] K.H. Kim and D.N. Lee, Acta Mater., 49, 2583-2595, 2001.
[7] J.P. Lee, M.Y. Huh and O. Engler, in preparation.
[8] V. Randle and O. Engler, Introduction to Texture Analysis, Macrotexture, Microtexture and Orientation Mapping, Gordon and Breach. Amsterdam, 2000.
[9] M.Y. Huh, K.R. Lee and O. Engler, Int. J. Plasticity, 20, 1183-1197, 2004.
[10] DEFORM2D, Ver. 7.1, Scientific Forming Technologies Cooperation, Columbus, OH, 2001.